Cooperative Atom-Light Interaction in a Blockaded Rydberg Ensemble

J. D. Pritchard,* D. Maxwell, A. Gauguet, K. J. Weatherill, M. P. A. Jones, and C. S. Adams†

Department of Physics, Durham University, Rochester Building, South Road, Durham DH1 3LE, United Kingdom

(Received 21 June 2010; published 5 November 2010)

By coupling a probe transition to a Rydberg state using electromagnetically induced transparency (EIT) we map the strong dipole-dipole interactions onto an optical field. We characterize the resulting cooperative optical nonlinearity as a function of probe strength and density. We demonstrate good quantitative agreement between the experiment and an N-atom cooperative model for $N = 3$ atoms per blockade sphere and the $n = 60$ Rydberg state. The measured linewidth of the EIT resonance places an upper limit on the dephasing rate of the blockade spheres of <110 kHz.

DOI: 10.1103/PhysRevLett.105.193603 PACS numbers: 42.50.Nn, 32.80.Rm, 34.20.Cf, 42.50.Gy

Strong dipole-dipole interactions, manifest as the dipole blockade mechanism [1], make Rydberg atoms attractive candidates for studies of quantum many-body physics and applications in quantum information [1–3]. The blockade mechanism suppresses multiple Rydberg excitations within a volume $(4/3)\pi r_b^3$, where the blockade radius r_b is typically of the order of a few microns. Experimental evidence of blockade is provided by the observation of the suppression of Rydberg excitation [4–7] and a collective enhancement of the transition dipole by a factor of $\sqrt{N}$ where N is the number of atoms in a blockade sphere [7–9]. This collective effect has been used to realize both atomic entanglement [10] and quantum gates [11]. Strong dipole interactions in Rydberg ensembles also open the possibility of manipulating nonclassical states of light [1], for example, single photon sources [3,12,13] or photonic phase gates [14]. One can use electromagnetically induced transparency (EIT) [15] to map the properties of the Rydberg states onto a strong optical transition [16]. This technique, coupled with the sensitivity of Rydberg states to electric fields, has been used demonstrate a giant dc Kerr effect [17] and measure electric fields close to surfaces [18]. Introducing strong dipole-dipole interactions into the atom-light interaction means that each atom can no longer be treated independently. Instead, correlations between atoms must be considered leading to a cooperative effect. As the dissipative component of the dipole-dipole interactions leads to superradiance [19], dipole-dipole induced nonlinearities have so far only been observed in an up conversion process [20]. However, for Rydberg systems in the blockade regime the superradiance is reduced.

In this Letter we demonstrate a cooperative atom-light interaction due to dipole blockade of the Rydberg state in an ultracold atomic ensemble. The effect of strong interactions between Rydberg pairs is mapped onto an optical transition using EIT [15,16] resulting in an optical nonlinearity. As EIT probes a dark state consisting of a superposition of the ground and Rydberg states, the line shape is sensitive to the coherence of the blockaded ensemble. We observe no additional dephasing of the dark state as the strength of the optical field, and hence the blockade effect, is increased. This result is inconsistent with a theoretical description of individual atoms coupled to a mean field, where one finds that the modification of the dark state due to interactions is always accompanied by dephasing and level shifts [21]. We show that a cooperative model describing the dynamics of the full N-atom system coupled to a classical light field provides good quantitative agreement for $N = 3$.

Our experiments are performed on a laser cooled ^{87}Rb atom cloud using the experimental setup described in [22] and shown schematically in Fig. 1(a). Atoms are loaded into a magneto-optical trap for 1 s, reaching a temperature of 20 μK. Atoms are then prepared in the $5s\ ^2S_{1/2}|F = 2, m_F = 2\rangle$ state ($|g\rangle$) by optical pumping. By varying the optical pumping duration, the fraction of atoms in $F = 2$ and hence the density in state $|g\rangle$ can be controlled without changing the cloud size. EIT spectroscopy is performed using counterpropagating probe and coupling lasers focused to $1/e^2$ radii of 12 and 66 μm, respectively. The coupling laser is frequency stabilized to the $5p\ ^2P_{3/2}$ $F' = 3 \rightarrow ns^2S_{1/2}$ transition using an EIT locking scheme [23]. The probe laser drives the $5s\ ^2S_{1/2}\ F = 2 \rightarrow 5p^2P_{3/2}$ $F' = 3$ transition and is scanned across the resonance from $\Delta_p/2\pi = -20 \rightarrow +20$ MHz in 500 μs. The probe and coupling lasers are circularly polarized to drive $\sigma^+ - \sigma^-$ transitions, maximizing the transition amplitude to the Rydberg state. Probe powers in the range 1 pW to 5 nW were used to explore the optical nonlinearity. The transmission is recorded using a single photon counting module. For each power, the experiment is repeated 100 times to build up a transmission histogram. The width of the atom cloud along the probe axis ℓ was measured by fluorescence imaging of the cloud after preparation in $F = 2$, giving $\ell = 1.4 \pm 0.1$ mm. To measure the density of atoms in the probe beam, the transmission data are recorded with the coupling laser off. The spectra are fitted using the analytic absorption profile for a two-level atom [24] to extract both the density and the effective Rabi frequency due to the saturation of the transition and Gaussian intensity profile. We obtain a

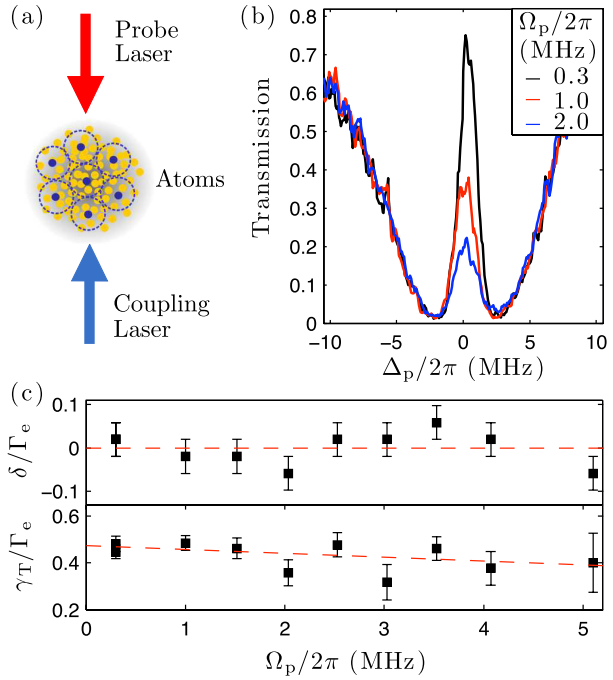

FIG. 1 (color online). (a) Schematic of experiment. EIT spectroscopy is performed on an ultracold ^{87}Rb atom cloud. (b) Suppression of transparency on resonance for coupling to $60S_{1/2}$ for increasing probe Rabi frequency Ω_p at a density $\rho = 1.2 \pm 0.1 \times 10^{10}$ cm^{-3}. (c) Detuning, δ, and width, γ_T, of EIT resonance as a function of Ω_p in units of the excited state width $\Gamma_e = 2\pi \times 6$ MHz, showing no dephasing and no resonance shift.

peak density of $\rho = 1.2 \pm 0.1 \times 10^{10}$ cm^{-3} giving around 7000 atoms in the interaction region.

Figure 1(b) shows EIT spectra as a function of probe Rabi frequency Ω_p for coupling to the $60S_{1/2}$ Rydberg state. As the probe Rabi frequency is increased, there is a dramatic suppression of transmission on the two-photon resonance from 75% to 20%. This intensity dependent transmission on resonance gives an optical nonlinearity. The effect saturates at $\Omega_p/2\pi = 5$ MHz. From the line shape the detuning (δ) and the FWHM (γ_T) of the two-photon resonance are extracted as a function of Ω_p, see Fig. 1(c). This shows there is neither a broadening nor a detuning of the EIT feature to accompany the suppression. The absence of a shift or broadening is significant, as it rules out inhomogeneous broadening mechanisms such as Stark shift due to ions or van der Waals dephasing of the Rydberg state [25].

The observation of suppression without shift or broadening is explained by considering the dipole-dipole interactions between Rydberg atoms [26]. For S states the long-range dipole-dipole potentials have the form $V(R) = -C_6/R^6$, where R is the interatomic separation and $C_6 < 0$ [27]. We consider a many-body system of N atoms, where each pair is coupled via the dipole-dipole interaction, shown schematically in Fig. 2(a). The resulting N-atom Hamiltonian $\hat{\mathcal{H}}_N$ is given by

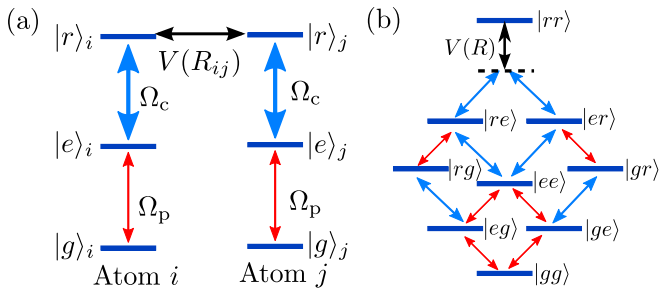

FIG. 2 (color online). Schematic of exact N-atom interaction model where all pairwise dipole-dipole interactions between atoms i and j are included. (b) Energy levels for $N = 2$ atom model. The dipole-dipole interaction term $V(R)$ acts to detune the doubly excited state off resonance, leading to blockade.

$$\hat{\mathcal{H}}_N = \sum_i^N \hat{\mathcal{H}}^{(i)} - C_6 \sum_{j<i} \frac{\hat{P}_{rr}^{(i)} \hat{P}_{rr}^{(j)}}{R_{jj}^6}, \tag{1}$$

where $\hat{\mathcal{H}}^{(i)}$ is the single atom Hamiltonian describing the coupling to the probe and coupling field acting on atom i and $\hat{P}_{rr}^{(i)} = |r\rangle_{ii}\langle r|$ is the projector onto the Rydberg state of the ith atom. For a given set of parameters the temporal evolution is calculated from the master equation $\dot{\hat{\sigma}} = i/\hbar[\hat{\sigma}, \hat{\mathcal{H}}_N] - \hat{\gamma}$ where $\hat{\sigma}$ is the $3^N \times 3^N$ density matrix for the N atom system and γ is the decoherence matrix, including the dephasing due to finite laser linewidth. The susceptibility, and the transmission, is calculated by summing over all the coherence terms in the density matrix between states that are coupled by the probe laser.

The effect of dipole-dipole interactions on the two-photon resonance can be seen from considering the simplest case of $N = 2$, shown in Fig. 2(b). In the absence of interactions [$V(R) = 0$] the system evolves into the following eigenstate on the two-photon resonance:

$$|D\rangle = \frac{\Omega_c^2|gg\rangle - \sqrt{2}\Omega_p\Omega_c|gr\rangle^+ + \Omega_p^2|rr\rangle}{\Omega_p^2 + \Omega_c^2}, \tag{2}$$

where $|gr\rangle^+ = (|gr\rangle + |rg\rangle)/\sqrt{2}$, Ω_c is the coupling Rabi frequency and the relative phase between the lasers has been neglected. This is a dark state as it is not coupled to the probe laser, leading to the observed transparency.

Dipole-dipole interactions between the Rydberg states modify this dark state by suppressing excitation of $|rr\rangle$ when $V(R) > \gamma_T$ due to blockade [1]. The resulting state can no longer be written as a product state and involves the components $|gg\rangle$, $|ge\rangle^+$, $|gr\rangle^+$, and $|er\rangle^+$. Because of the rapid decay of state $|e\rangle$ this state differs from the eigenstate found in [28]. The physical interpretation of this result is that the system is in a superposition where only one atom can be excited to the Rydberg state and thereby contribute to the EIT dark state, while the other acts as a two-level atom which couples resonantly to the probe field. This leads to a suppression of transmission on resonance. The blockade forms a collective state where the single Rydberg excitation

is shared between the two atoms. As more atoms are included in the blockade sphere, the single excitation is shared across a larger number of atoms, further suppressing the transmission on resonance. The resulting nonlinearity is sensitive to the photon statistics of the probe field; however, below we focus on classical fields.

We demonstrate the scaling of the nonlinearity with number of atoms in each blockade sphere by changing both the density and the principal quantum number n. In an ordinary nonlinear medium, the optical response scales linearly with density as each optical dipole is independent. For a cooperative effect due to dipolar interactions, the optical response is now proportional to the number of atoms in a blockade sphere, leading to a nonlinear scaling with density. Figure 3 shows the optical depth on resonance as a function of density for $60S_{1/2}$ and $54S_{1/2}$ for both strong and weak probe powers. To remove the trivial linear response with density the optical depth is scaled by the value with coupling laser off. In the weak probe regime, the resonant eigenstate is equivalent to $|D\rangle$ and no nonlinear scaling is observed. For the strong probe data, there is a second-order scaling with density, consistent with increased suppression due to an increase in the number of atoms in each blockade sphere. Taking into account the scaling of C_6 and Ω_c with n, the number of atoms in a blockade sphere should scale as $N \propto n^{6.25}$. The ratio of N for $60S$ to $54S$ is 2.0, while the ratio of the linear fit gradients gives a ratio of 2.6 ± 0.7. This is consistent with the blockade scaling, showing the tunability of the cooperative optical nonlinearity with principal quantum number.

To reproduce the data shown in Fig. 1 it is necessary to solve the many-body Hamiltonian for the average number of atoms in each blockade sphere. For the $60S_{1/2}$ state, the van der Waals coefficient is $C_6 = -140$ GHz μm^6 [29], which for $\gamma_T/2\pi = 3$ MHz gives a blockade radius $r_b = \sqrt[6]{C_6/\gamma_T} = 6$ μm. For a density of 1.2×10^{10} cm^{-3} this gives an average of $\bar{N} = 11$ atoms in each blockade sphere. As a full solution of Eq. (1) for large N is demanding, previous work on N-atom blockaded systems have focused on a mean-field description [4,30–32]. However, a mean-field approach is insufficient to reproduce the experimental observations shown in Fig. 1 as the average interaction experienced by each atom by its neighbors contributes to blue shift of the Rydberg state. This leads to both broadening and a shift of the EIT line shape when summing over each atom [21]. No dephasing is observed in our experiment because the blockade suppresses multiple Rydberg excitations and consequently van der Waals dephasing is also suppressed.

To obtain quantitative agreement with the full N-atom model we reduce the density to $0.35 \pm 0.03 \times 10^{10}$ cm^{-3} to give an average of $\bar{N} = 3$ atoms per blockade sphere. Transmission data for $\Omega_p/2\pi = 0.1$ to 3.2 MHz is shown in Figs. 4(a)–4(c), again showing suppression of the resonant transmission but by a smaller amount as the number of

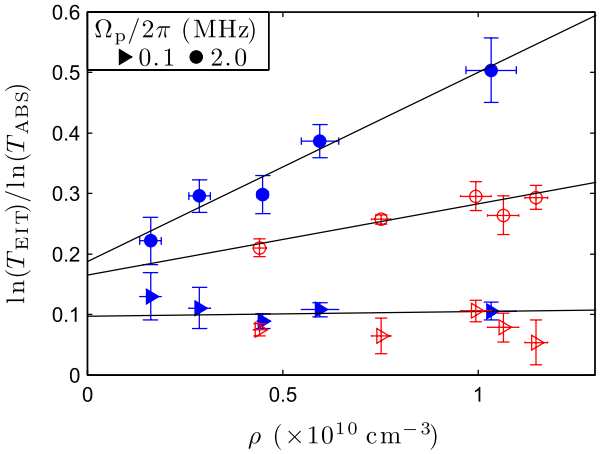

FIG. 3 (color online). Optical depth $[-\ln(T_{EIT})]$ as a function of density for $60S_{1/2}$ (▶, ●) and $54S_{1/2}$ (▷, ○) for weak and strong Ω_p, respectively, scaled by probe-only optical depth $[-\ln(T_{ABS})]$ to remove trivial linear scaling. Strong probe data reveal a second order density scaling consistent with a cooperative optical nonlinearity. Comparison of the gradients for $60S_{1/2}$ and $54S_{1/2}$ gives a ratio of 2.6 ± 0.7.

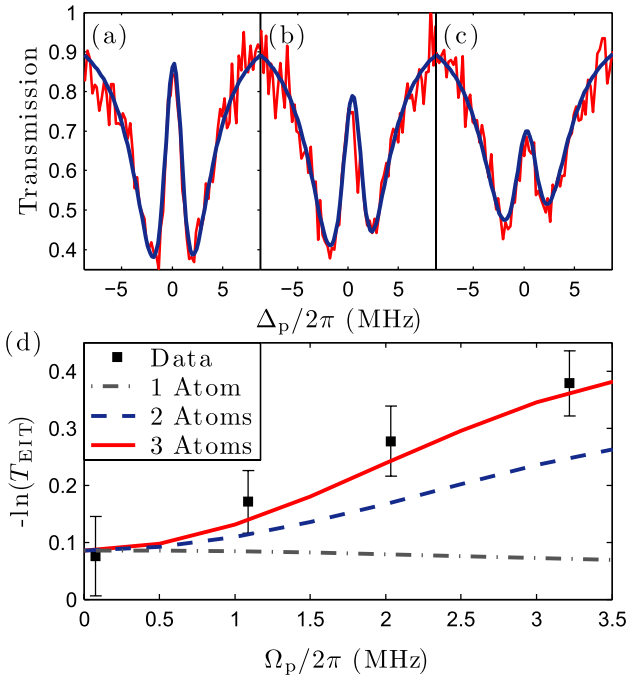

FIG. 4 (color online). Comparison of N-atom model to transmission data at a density of $\rho = 0.35 \pm 0.03 \times 10^{10}$ cm^{-3} with $\bar{N} = 3$. Traces (a)–(c) show spectra recorded at $\Omega_p/2\pi = 1.0$, 2.0, 3.2 MHz, respectively, with the three-atom model plotted on top (thick line). (d) Optical depth on resonance as a function of Ω_p compared to model for $N = 1$, 2, and 3 atoms. Good qualitative agreement is obtained for $N = 3$ to both resonant transmission and line shape. All curves calculated using $\Omega_c/2\pi = 3.8$ MHz and $V(R)/2\pi = 15$ MHz with linewidths of the probe laser and two-photon transition of 0.2 and 0.11 MHz, respectively.

atoms per blockade is reduced. Also shown on the data is the transmission calculated using the many-body model for $N = 3$. Model parameters are determined by matching the single atom model to the weak probe transmission for $\Omega_p/2\pi = 0.1$ MHz, yielding the coupling Rabi frequency and linewidths of the probe laser and two-photon resonance of 3.8, 0.2, and $0.1(\times 2\pi)$ MHz, respectively, consistent with experimental parameters. Transmission traces are then calculated changing only Ω_p. There is only one free parameter in the model, which is the interaction strength V. For the model traces in Fig. 4 calculations were performed using $V/2\pi = 15$ MHz; however, the model is insensitive to V once the blockade condition ($V > \gamma_T$) is met. The model shows very good quantitative agreement with the data, reproducing both the suppression on resonance and the EIT line shape. Figure 4(d) shows the optical nonlinearity by plotting the optical depth on the two-photon resonance as a function of Ω_p compared to the model for $N = 1$, 2, and 3. The small decrease with Ω_p observed for $N = 1$ is due to the system being driven faster relative to the dephasing caused by finite laser linewidth. Comparing this to the curves for $N = 2$ and 3 shows that the transmission is strongly modified compared to the case for a single atom, with a good agreement to the $\bar{N} = 3$ data as expected.

The results of Figs. 1(c) and 4 show that EIT is sensitive to the coherence of the blockaded ensemble, as only by considering the coherence terms of the complete many-body system is it possible to reproduce the suppression of transmission without introducing broadening. The linewidth of the EIT is a function of the broadening due to the coupling Rabi frequency and the relative laser linewidth of the two-photon transition. Fitting the line shape for the weak probe data in Fig. 1(a) gives a laser linewidth of 110 ± 50 kHz. As the probe Rabi frequency is increased, the system evolves into an ensemble of blockaded regions on resonance. Dephasing between neighboring blockade spheres would lead to broadening of the EIT resonance, appearing as an effective increase in the relative laser linewidth of the two-photon transition as Ω_c remains constant. Since no additional broadening is observed in the experiment, this places an upper limit on the dephasing rate of each blockade sphere of <110 kHz for $60S_{1/2}$.

In summary, we explore the effects of dipole-dipole interactions between Rydberg atoms on light propagation. By mapping the strong interactions onto an optical field, a novel cooperative optical nonlinearity is observed. This differs from other cooperative effects such as superradiance, where the cooperativity is mediated by the optical field. Instead, the cooperativity arises from long-range dipole-dipole interactions between Rydberg states that is observed as a backaction on the probe field. As the optical response of each atom is significantly modified by its proximity to neighboring atoms, the dynamics can only be described by treating all N atoms in each blockade sphere. We show excellent quantitative agreement between experiment and theory for three atoms per blockade, and verify the expected density scaling with the strength of the van der Waals interaction. By probing the coherence of the blockaded system we place an upper limit on the dephasing rate of each blockade sphere of <110 kHz, enabling potential applications in quantum optics. Future work will focus on demonstrating the use of the nonlinearity to create nonclassical states of light, and the development of a single photon source based on a single blockaded ensemble.

We thank M. Müller and I. Lesanovsky for help with elucidating the theoretical origin of the suppression effect. We are also grateful M. Fleischhauer, R. M. Potvliege, I. G. Hughes, and T. Pfau for stimulating discussions, and acknowledge support from the U.K. EPSRC.

*j.d.pritchard@durham.ac.uk
†c.s.adams@durham.ac.uk

[1] M. D. Lukin *et al.*, Phys. Rev. Lett. **87**, 037901 (2001).
[2] D. Jaksch *et al.*, Phys. Rev. Lett. **85**, 2208 (2000).
[3] M. Saffman and T. G. Walker, Phys. Rev. A **66**, 065403 (2002).
[4] D. Tong *et al.*, Phys. Rev. Lett. **93**, 063001 (2004).
[5] K. Singer *et al.*, Phys. Rev. Lett. **93**, 163001 (2004).
[6] T. Vogt *et al.*, Phys. Rev. Lett. **97**, 083003 (2006).
[7] R. Heidemann *et al.*, Phys. Rev. Lett. **99**, 163601 (2007).
[8] A. Gaëtan *et al.*, Nature Phys. **5**, 115 (2009).
[9] E. Urban *et al.*, Nature Phys. **5**, 110 (2009).
[10] T. Wilk *et al.*, Phys. Rev. Lett. **104**, 010502 (2010).
[11] L. Isenhower *et al.*, Phys. Rev. Lett. **104**, 010503 (2010).
[12] D. Porras and J. I. Cirac, Phys. Rev. A **78**, 053816 (2008).
[13] L. H. Pedersen and K. Mølmer, Phys. Rev. A **79**, 012320 (2009).
[14] I. Friedler *et al.*, Phys. Rev. A **72**, 043803 (2005).
[15] K.-J. Boller, A. Imamoğlu, and S. E. Harris, Phys. Rev. Lett. **66**, 2593 (1991).
[16] A. K. Mohapatra, T. R. Jackson, and C. S. Adams, Phys. Rev. Lett. **98**, 113003 (2007).
[17] A. K. Mohapatra *et al.*, Nature Phys. **4**, 890 (2008).
[18] A. Tauschinsky *et al.*, Phys. Rev. A **81**, 063411 (2010).
[19] R. H. Dicke, Phys. Rev. **93**, 99 (1954).
[20] M. P. Hehlen *et al.*, Phys. Rev. Lett. **73**, 1103 (1994).
[21] H. Schempp *et al.*, Phys. Rev. Lett. **104**, 173602 (2010).
[22] K. J. Weatherill *et al.*, J. Phys. B **41**, 201002 (2008).
[23] R. P. Abel *et al.*, Appl. Phys. Lett. **94**, 071107 (2009).
[24] R. Loudon, *The Quantum Theory of Light* (OUP, UK, 2008), 3rd ed.
[25] M. Gross and S. Haroche, Phys. Rep. **93**, 301 (1982).
[26] M. Müller, I. Lesanovsky, and P. Zoller (private communication).
[27] T. Amthor *et al.*, Phys. Rev. A **76**, 054702 (2007).
[28] D. Møller, L. B. Madsen, and K. Mølmer, Phys. Rev. Lett. **100**, 170504 (2008).
[29] K. Singer *et al.*, J. Phys. B **38**, S295 (2005).
[30] H. Weimer *et al.*, Phys. Rev. Lett. **101**, 250601 (2008).
[31] A. Chotia *et al.*, New J. Phys. **10**, 045031 (2008).
[32] U. Raitzsch *et al.*, New J. Phys. **11**, 055014 (2009).